Simulation of Mass Fire-Spread in Urban Densely Built Areas Based on Irregular Coarse Cellular Automata

Sijian Zhao, State Key Laboratory of Earth Surface Processes and Resource Ecology, Beijing Normal University, Beijing 100875, China

Sijian Zhao*, Academy of Disaster Reduction and Emergency Management, Ministry of Civil Affairs & Ministry of Education, Beijing Normal University, No. 19 Xinjiekouwai Street, Beijing 100875, China

Sijian Zhao, Key Laboratory of Environmental Change and Natural Disaster, Ministry of Education of China, Beijing Normal University, Beijing 100875, China

Sijian Zhao, Beijing Research Center of Urban Systems Engineering, Beijing 100089, China

Abstract. Mass fire-spread is a potential threat to some densely built urban areas by its devastating destructions. Especially in case of a large earthquake when multiple fires break out simultaneously, fire-spread hazard is likely to overwhelm fire-fighting capabilities and enlarge damage area. To explore fire-spread behavior and assess its damages, a simulation model of fire-spread in densely built urban areas is developed. Cellular Automata (CA) is a Bottom-up dynamics model that can reproduce a complicated phenomenon by setting up simple rules in a cell space. However, the traditional grid-based cells of CA are not suitable for modeling building-to-building fire-spread behavior. Therefore, an irregular coarse CA schema is proposed in this paper. Two sub-processes are involved urban mass fire-spread, i.e. (I) fire-developing in a single building and (II) fire-spread among buildings. When a fire is developing in a single building, the building will experience 5 fire stages along time, which become the states of cell. While fire spreads among buildings, there are 2 spread patterns: (I) short-range direct flame contact, radiation and convection spread and (II) long-range firebrand spotting spread. In relation to the 2 spread patterns, 2 sets of neighborhoods and rules of CA are formulated respectively. To verify the newly developed model, 100 times of individual random simulations for a real site fire-spread in Kobe City after Hanshin Earthquake (1995, Japan) are performed using an integrated GIS-CA-fire tool developed in the paper. Comparing the simulation results with the local observations, the general feature of fire-spread is found similar, and it is proved that the newly developed model is reliable to simulate urban fire-spread. Furthermore, based on the simulated results, a loss assessment model is formulated to calculate economic and life losses after fire-spread.

Keywords: Urban mass fire-spread, Simulation, Irregular coarse CA, Short-range spread, Long-range spread

---

* Correspondence should be addressed to: Sijian Zhao, E-mail: zhaosijian@ires.cn

1. Introduction

Mass fire-spread is a dangerous urban disaster for its great potential destructions. Especially, in some densely built cities, such as Japan and China, with large numbers of wooden or wooden frame buildings, once an ignition appears in a building, fire would easily propagate to adjacent buildings one after another. Mass fire-spread often appears as a result of warfare or natural disaster [1]. Wartime mass fires such as those in Hamburg, Germany and Hiroshima, Japan are widely discussed in history books or popular presses [1]. Natural disaster, mainly earthquake, is a major cause of the recent urban mass fire-spread hazards. Historically, United States and Japan have frequently experienced such post-earthquake fires and suffered from great damages [2, 3]. For example, fires in Chicago (USA, 1871) after shake lasted for 3 days, burning down above 17,000 buildings and causing over 300 fatalities; the conflagrations accompanied by the San Francisco Earthquake (USA, 1906) spread over 521 blocks, of which 508 ones were completely burnt up; the fires after Kanto Earthquake (Japan, 1926) toke away over 100,000 lives and spread about 38,000,000 m^2 area, in which almost 70% buildings were completely burnt down; the Hanshin Earthquake (Japan, 1995) induced 138 fires during the following 3 days, causing about 660,000 m^2 burnt regions, more than 6900 burnt houses, and over 500 fatalities by fire [2, 3]. All above cases indicate that urban mass fires induced by warfare or earthquake would bring devastating damages to human beings, therefore, sufficient attentions should be paid to avoid the recurrence of these historical calamities. For this purpose, this paper carries out a deep analysis on the process of urban mass fire-spread, and then a simulation model and a tool is developed to study its complicated behaviors. The model and tool will be further applied in fire loss assessment and decision-making for urban fire hazard mitigation.

Urban mass fire-spread is a particularly complicated phenomenon. At present, most of the researches on fire-spread focus on fire spreading within one room (so-called 'compartment fires') and very limited researches have been performed on urban inter-building fire-spread. Moreover, more work has been performed on wild land fire-spread [4], but this work is of limited applicability to the urban scenario. In Japan, several attempts have been made in developing models for prediction of urban fire-spread behaviors. Such a model was firstly proposed by Hamada in 1951 [5], in which the rate of fire-spread was formulated empirically as the function of macroscopic parameters of the environment, such as wind speed, building scale, building-to-building separation, construction types, etc. Subsequently, some experts, such as Suzuki and Hishida, Horiuchi, Fujita, Scawthorn and Sakai modified the Hamada model based on more detailed historical fire data [6]. However, since their models were all formulated on historically data, some empirically statistical parameters were inevitably involved, which may lose validity through time as the conditions of urban environment, such as fire protection performance of individual buildings or urban structure in general, may change dramatically. Recently, Himoto and Tanaka [7–9], and Lee and Davidson [10] developed the physically based fire-spread models, but their models are so complicated in calculation that it is unsuitable for rapid simulation of fire-spread in large

urban areas. Additionally, Cousins et al. [11] and Ohgai et al. [12] used cellular automata (CA) with 3 m × 3 m grid cells to model urban fire-spread. But in relation to modeling building-to-building fire-spread, regular grid cell is no suitable. In order to avoid the mentioned disadvantages, this paper aims to develop a new simulation model and tool by using irregular coarse CA to reproduce the complicated phenomenon of urban mass fire-spread.

The remainder of this paper is structured as follows. Section 2 makes a deep analysis on the process of urban fire-spread and explores its inherent mechanisms. Then, the principle of CA model is briefly introduced in Section 3. Section 4 describes how to use irregular coarse CA to model urban fire-spread and illustrates its execute flow in detail. After that, a seamlessly integrated GIS-CA-fire tool is developed and its main user interfaces are introduced in Section 5. To verify the newly developed model, the fire-spread at a real site in Kobe City of Japan is simulated with GIS-CA-fire tool and the simulated results are compared with local observations in Section 6. Based on the new model and tool, Section 7 further formulates a loss assessment model induced by fire-spread. Finally, a summery and several issues for future work are stated in Section 8.

2. The Process of Urban Mass Fire-Spread

Urban mass fire-spread includes 2 sub-processes: (I) fire-development in a single building and (II) building-to-building fire-spread.

2.1. Fire-Development in a Single Building

Generally, *Ignition* may initially occur in a room of building. If no one discovers, the ignition will grow up at a rate depending on several factors, such as the type of fuels, access to oxygen, room's configuration etc. After the short-term growing up, the initial ignition will burst into *flashover* period, which is a rapid transition from growth period to a fully developed fire, resulting in the total surface of the combustible materials being involved in fire [13]. Soon after flashover, the fire will step into *full-development* stage. At this stage, the rate of heat release and average temperature inside fire room reach the peak, and the fire will spread to other rooms and levels through a variety of possible paths including the horizontal spreading through the combustible doors and walls; and the vertical spreading through elevators, stairs, vent-pipes and outside windows. Even worsely, if under the situation of blast or shake, the fire protection systems (fire alarms, auto-sprinkle systems, fire doors etc.) inside building may be damaged seriously to lose functions to inform and stop fire-spread. Meanwhile, fire-fighting activities from local fire departments may be delayed due to the chaos after war or quake. Therefore, in such cases, the room fires cannot be suppressed timely and easily spread to the whole building, becoming *structure fire*. In common, under the background of war or earthquake, if the fire becomes large enough to flash over a room, it is usually assumed that the entire building will be lost in the fire [1]. Once becoming a structure fire, it has the strong capability to spread fire to its adjacent buildings. When the fire building reaches the fireproof limit, it may *collapse* and the fire intensity

will go down gradually. Especially, the incombustible debris from collapsed building may cover fuels, which will lead to sharp declination of fire intensity or even final fire extinguishment [12]. In summary, when an ignition breaks out in a room, the building will experience 5 key fire stages in sequence, i.e. *ignition, flashover, full development, structure fire* and *collapse*.

2.2. Building-to-Building Fire-Spread

When a fire is developing within a single building, it will simultaneously spread to the adjacent buildings. The building-to-building fire-spread occurs in several manners or a combination of manners [1]. According to historical records of urban mass fires following war or earthquake, the manners of fire spread among buildings include (I) direct flame contact, (II) radiative heating, (III) thermal plume heating and (IV) firebrand spotting (Figure 1) [14]. Among them, radiation is the primary fire-spread manner. When a fire develops in a building, radiation is emitted from the fire room through external windows and the flames projected out of the windows. Nearby buildings are likely to be ignited once the received radiation flux reaches a critical level. In addition, a large amount of hot gases, so-called plume, are released from fire rooms and then flow into the sky over the city through windows. In the presence of wind, the plume can tilt on the leeward side and flow long distances from the fire building. The heat from the thermal plume can also ignite buildings because of its high temperature. Moreover, during the
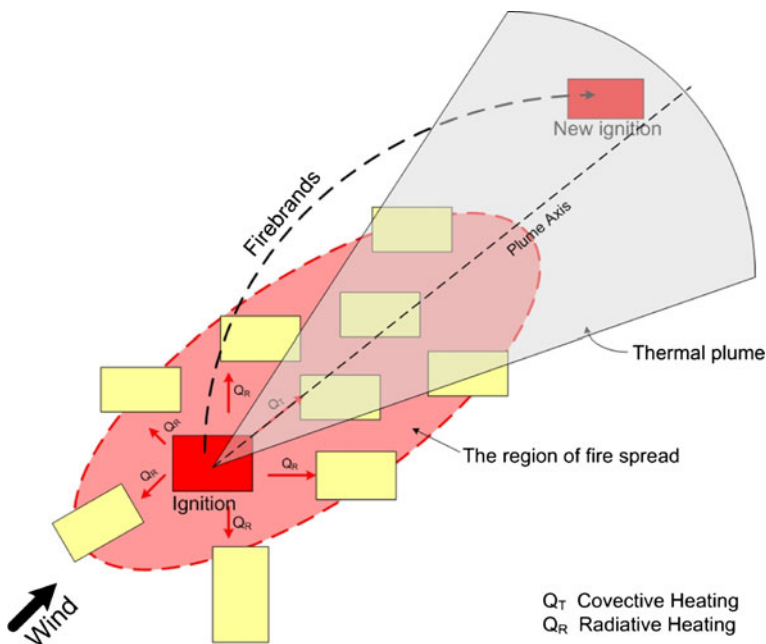
Figure 1.   Manners of building-to-building fire spread.

mass fires in the urban areas, it is often observed that pieces of solid burning fuels (such as brands or embers) can be lifted by the buoyant plume, blown by the wind and deposited at a large distance [1]. New ignition occurs if the brands or embers keep burning after they land on the ground. Spread from firebrands is a manner of fast fire-spread, because it can result in 'spotting' at significant distances from the fire front and contribute significantly to the ability of fire to jump firebreaks [1].

According to the spread distance, the building-to-building fire-spread can be further divided into 2 patterns: short-range and long-range spreads [15]. Short-range spread refers to the short-distance spread caused by direct flame contact, radiation and thermal plume, while long-range spread refers to the jump spread from firebrand spotting. Such 2 spread patterns were used in the following fire spread modeling.

3. Cellular Automata Model

Cellular Automata (CA) was firstly proposed by John von Neumann and Stanislaw Ulam in the 1940s for self reproduction in biological systems. It is a bottom-up dynamic system, which is discrete in space and time, operates on a uniform finite or infinite regular lattice and is characterized by local interactions. CA is mainly composed of *cells*, *cellular space*, *neighborhoods*, and *rules*. Each cell, as an element, is associated with a state given in a discrete set and is updated based on the previous states of its immediate neighboring cells according to a set of local rules.

The basic definition of CA is given as following [16, 17]:

Definition Let F be a cellular space and S be a finite and discrete state set, a cellular automaton A is locally defined by the couple:

$$A = (f, N) \tag{1}$$

where

- N is the so-called neighborhood, which may be given as a mapping:

$$N : F \rightarrow F^n$$
$$c \rightarrow N(c) = (c_1, c_2, \ldots, c_n) \tag{2}$$

and describes the local interactions between cells in F.

- f is a local transition function which calculates the state of a cell $c \in F$ at time $t + 1$ (denoted by $s_{t+1}(c)$) based on the states of its neighborhood $N(c)$ at time $t(S_t(N(c)) = \{S_t(c_i), c_i \in N(c)\})$. It can be expressed by:

$$f : F^n \rightarrow F$$
$$s_t(N(c)) \rightarrow s_{t+1}(c) = f(s_t(N(c))) \tag{3}$$

The cell's neighborhood can be given as below:

$$N(c) = \left\{ c' \in F \mid \|c' - c\|_i \leq r \right\} \tag{4}$$

where $\|c\|_i$, $i = 1,\ldots,\infty$ indicates the sum and the maximum of the absolute value of the components of cell c respectively. The corresponding neighborhood of radius r is called von Neumann and Moore. We denote by $n = |N(c)|$ the cardinality of the set $N(c)$, which defines the neighborhood size.

CA have generated a great deal of interests since the early 1960s when John Conway created the 'Game of life' and are now extensively studied for modeling and simulation of real spatial and temporal processes in a wide variety of application domains: mostly in the context of complex physical, ecological, biological or engineering systems (fluid dynamics, traffic, plant growth, fire or epidemic propagation, etc.) [18–21]. They are also applied in computability theory and mathematics. They can be viewed as an abstraction of massively parallel computers [22].

## 4. Urban Fire-Spread Modeling with CA

This section describes urban fire spread modeling with the use of irregular coarse CA, including cells, cell states, neighborhoods, rules, and the execute process of simulation.

4.1. Cells

Cell is a basic analytical unit in CA model. In general, CA model divides the study area, i.e. cellular space, into lattices (grids) as cells. Cell's size is mainly determined by the situation, and each cell has the characteristics of the area which it belongs to. Meanwhile, each cell has only one state of several limited states according to the local circumstances. The state would change with time. Cells can impact the states of neighboring cells by applying the rules.

For modeling fire-spread with CA, the urban region is divided into equal-size grids, namely regular fine cells in this paper (Figure 2a). But this type of cell is not suitable for fire-spread modeling due to the following 3 disadvantages.

- *Has Difficulty in the Size Determination of Cell.* A rational cell size cannot be easily determined because both representation and computational efficiency need to be considered together. If the size were too large, the cell would lose representation of real circumstance. For example, a 20 m × 20 m cell may cover two or more buildings. As a result, simulation cannot reproduce the real fire-spread phenomena from one building to another. On the other hand, if the size were too small, there would be a dramatic increase in calculation time and volume of data.
- *Has Difficulty in the Characteristic Determination of Mixed Cell.* If urban region is divided into grids, it is unavoidable that two or more materials would exist in one grid. We call them mixed cells. To determinate mixed cell's characteristic, the area method and power method are widely used. The area method means
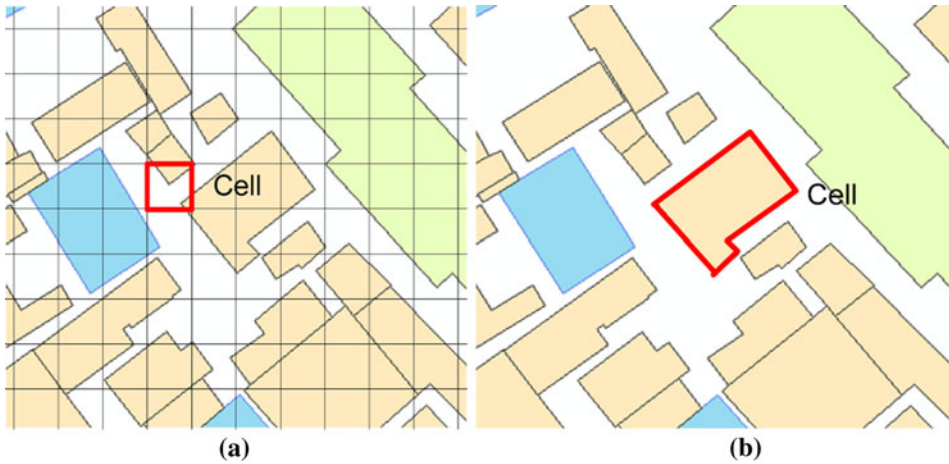
Figure 2.   Comparison of two types of cell schemas. (a) Regular fine cell and (b) irregular coarse cell.

that the material with the largest area determines the cell's characteristic. While with the power method, the cell's characteristic is determined by the most important material. No matter which one is used, the mixed cell can just approximately represent the local characteristics.

• *Cannot Reflect the Real Fire Stage of a Single Building*. As an ignition breaks out in a building, the building would experience different fire stages as an individual with time escape. However, when several grids all represent a building, different fire stages are likely to occur in different grids at the same time, which is irrational.

To avoid the disadvantages above, irregular coarse cell, i.e. a building as a cell directly (Figure 2b), is proposed to replace regular fine cell. Such cell can be easily picked out based on the layout of urban buildings to avoid dividing urban region into grids. On the other hand, the mixed cells will disappear and the cell's characteristics can be determined by its corresponding building's attributes directly. Moreover, irregular coarse cell can perfectly reflect the real fire stages of an individual building. In summary, it is a satisfying schema to use irregular coarse cell for urban fire-spread modeling with CA.

As for the cell's characteristics, both building attributes and weather conditions need to be considered. The building attributes consist of the structure type, damage type (by war or earthquake), floor area, stories, people density, construction value and inner property value. Among them, the first 3 attributes are closely related to the burning possibility of building and the last 4 attributes will be used for fire-induced losses calculation. The weather conditions refer to the wind speed and direction respectively, which will determine the speed, direction and range of fire spread.

4.2. Cell States

In corresponding to the 5 fire stages of a burnt building, there exist 6 states of cell (Table 1). State {0} is the original stage of cell, representing the building not burning yet but having the possibility of burning. Once the building catches fire, the state of cell changes to state {1}. With the elapsed time after ignition, the building experiences the stages of flashover, full development and structure in sequence. Correspondingly, cell state changes from {1} to {2} to {3} and finally to {4}. In each state of {2}, {3} and {4}, the ability of a cell to spread fire to other cells is different: state {2} has no ability to spread fire; state {3} has weak ability to spread fire; and state {4} has strong ability to spread fire. After a long-term intense burning, the building collapses and the fire self-extinguishes gradually. In this stage, cell state changes from {4} to {5} and has no ability to spread fire due to the sharp decrease of fire intensity.

In order to display the transition of states, a color symbol schema is chosen to represent 6 cell states (Table 1). In detail, white color is used for the original state {0}; a gradual red-color spectrum is used for the states {1}, {2}, {3} and {4} when fire developing in a building; grey color is used for state {5} when the building collapses or fire self-extinguishes.

Time interval t is a key parameter to measure the transition of cell states. Due to the difference of structure type, time intervals between states are greatly different. According to the fire-prevention performance, 3 types of structure, i.e. wooden, fire-prevention wooden and fireproof structures, are chosen to approximately represent urban building environment. In relation to these 3 structure types, the empirical values of time interval between states are given by experts as Table 2. Using time intervals above, the escaped time t_f from state {1} to {2} is equal to t_1; the escaped time t_d from state {2} to {3} is equal to $t_1 + t_2$; the escaped time t_s

Table 1
States and Symbols of a Cell in Corresponding to Fire Stages

Fire stage	State	Symbol	Explanation
Original stage	{0}		Not burning yet, but having the possibility of burning
Ignition	{1}		Catching fire, but having no ability to spread fire outside
Flashover	{2}		Self-developing, but having no ability to spread fire outside
Full development	{3}		Spreading inside building, having weak ability to spread fire outside
Structure fire	{4}		A whole building in fire, having strong ability to spread fire outside
Collapse	{5}		Collapse and extinguishment, having no ability to spread fire outside

Table 2
Time Intervals Between States in Corresponding to Three Types of Structures

Transition of states	Time interval (min)	Structure type		
		Wooden	Fire-pre wooden	Fire proof
$\{1\} \rightarrow \{2\}$	t_1	[4, 6]	[4, 6]	[4, 6]
$\{2\} \rightarrow \{3\}$	t_2	[5, 8]	[5, 8]	[5, 8]
$\{3\} \rightarrow \{4\}$	t_3	[10, 20]	[20, 30]	[30, 40]
$\{4\} \rightarrow \{5\}$	t_4	[20, 30]	[30, 40]	[50, 60]

Note: The time intervals above are given by the experts to be the default values, and they can be modified by users according to the real conditions of studied city.

from state $\{3\}$ to $\{4\}$ is equal to $t_1 + t_2 + t_3$; the escape time t_p from state $\{4\}$ to $\{5\}$ is equal to $t_1 + t_2 + t_3 + t_4$. The t_1, t_2, t_3 and t_4 are all randomly chosen in uniform from the ranges according to the structure type of a cell.
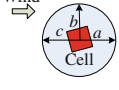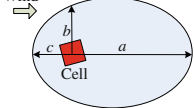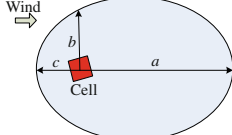
4.3. Neighborhoods

As mentioned in Section 2, building-to-building fire-spread has 2 main patterns, i.e. short-range and long-range fire-spreads. Corresponding to these 2 patterns, there exit 2 neighborhood settings described as below.

4.3.1. Short-Range Fire-Spread. Short-range fire-spread refers to the direct flame contact, radiative and convective spread leading to a relatively short spread distance comparing with firebrand spotting. According to the statistics of historical urban mass fires following famous earthquakes in Japan and US, the shape of short-range fire-spread nearly likes an ellipse with the fire cell located at the center of ellipse's semi-major. In such ellipse, 3 shape parameters *a*, *b* and *c* are used to represent the leeward-side, lateral-side and backward-side distances of fire-spread from a fire cell respectively. In addition, 2 wind parameters play important roles in shaping the ellipse, i.e. wind direction θ (in radians) determining the direction of ellipse's principle axis and wind speed *v* (m/s) determining the longest distance from the fire cell's center to the boundary of ellipse. Moreover, the parameter *d*, the length scale of cell calculated with the square root of cell's floor area $\sqrt{A}$, also affect the shape of ellipse.

To be specific, the ellipse's shape can be determined using parameters above as below (Table 3). In the presence of a slight wind, i.e. $v = 0$–5 (m/s), the shape of fire spread is a circle with *a*, *b* and *c* all taking the value of 3 + d/2 (m). In case of a big wind, i.e. $v = 5$–10 (m/s), the circle turns into an ellipse with *a* taking a value of 8.5 + d/2 (m), *b* taking a value of 2 + d/2 (m), and *c* taking a value of 2.5 + d/2 (m). Once a strong wind occurs, i.e. $v = 10$–15 (m/s), *a* takes a value of 12 + d/2 (m), *b* takes a value of 1 + d/2 (m), and *c* takes a value of 2 + d/2 (m). The wind with speed larger than 15 (m/s) is not considered in the current neighborhood setting for it is very rare in general cities.

Table 3
Neighborhood of Short-Range Fire-Spread

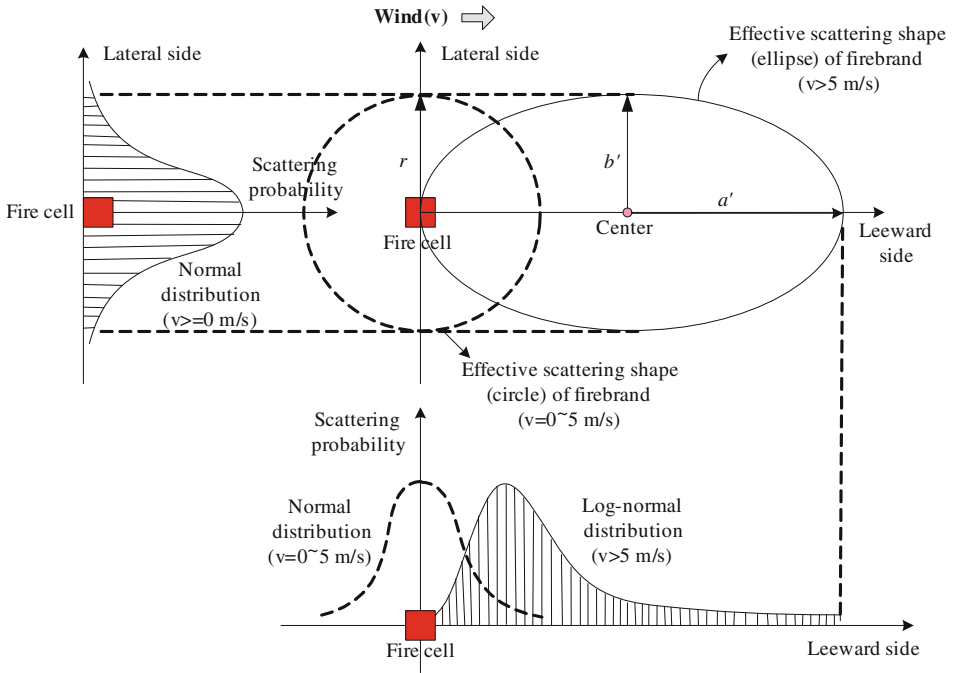| Wind type	Slight wind	Big wind	Strong wind
Wind velocity, v (m/s)	0–5	5–10	10–15
Neighborhood (Fire spread ellipse or circle)			
Parameters			
a (m)	3 + d/2	8.5 + d/2	12 + d/2
b (m)	3 + d/2	2 + d/2	1 + d/2

Note: The values of parameters are originally given from empirical fire-spread Hamada model and further modified based on the statistics of the fire-spread records after Kobe Earthquake (1995).

Once the spread ellipse (circle) is specified, all cells locating inside or intersecting with the ellipse (circle) become the short-range neighbors of a fire cell.

4.3.2. Long-Range Fire-Spread. Long-range fire-spread refers to the long distance fire-spread resulted from firebrand spotting. In case of an urban fire, enormous number of firebrands is released into the fire induced flow field. However, only a fraction of them actually causes the fire-spread as the occurrence of ignition by a firebrand depends on several conditions, such as the properties of firebrand, local-scale wind conditions, transport location, properties of target combustible, atmospheric conditions, etc. Of them, only 2 critical conditions, i.e. the local wind conditions and the transport location of a firebrand by wind, are considered in formulating the long-range neighborhood setting.

The scattering of a firebrand is not uniform because of its complicated transport trajectories by wind. According to Himoto and Tanaka [9], in the presence of wind, the scattering of a firebrand along the wind direction (i.e. leeward side) approximately satisfies as a log-normal distribution and the one along the orthogonal direction (i.e. lateral side) approximately satisfies as a normal distribution (Figure 3). For the sake of simplicity, it is also assumed that the effective scattering shape of a firebrand released from a fire cell is similar to an ellipse. While in the absence of wind or in a slight wind, the scatterings along the leeward and lateral sides all satisfy as a same normal distribution, and the effective scattering shape becomes a circle with the fire cell as its center (Figure 3).

As shown in Figure 3, 3 shape parameters are employed to shape the effective scattering ellipse (circle) of a firebrand released from a fire cell: a' is the half of ellipse's major-axis length, b' is the half of ellipse's minor-axis length and r is the length of circle's radius. Moreover, 2 wind parameters also affect the shape of scattering ellipse (circle): wind direction θ determines the direction of ellipse's major-axis and wind speed v determines the long-axis length of ellipse.

Figure 3.   Scattering distribution of a firebrand in leeward and lateral sides.

Table 4
Neighborhood of Long-Range Fire-Spread

Wind type	Slight wind	Big wind	Strong wind
Wind velocity, v (m/s)	0–5	5–10	10–15
Neighborhood (Scattering ellipse or circle of a firebrand)			
Parameters			
a' (m)	–	20	30
b' (m)	–	15	15
r (m)	15	–	–

Note: The values of parameters are estimated based on the investigation records of fires after Kobe Earthquake [14] and some research achievements [5, 6, 9].

To be specific, the shape of effective scattering ellipse (circle) can be further determined as Table 4. In a slight wind, i.e. $v = 0$–5 (m/s), the parameter r takes a value of 15 (m). In case of a big wind, i.e. $v = 5$–10 (m/s), the parameters a'

and b' take the values of 20 (m) and 15 (m) respectively, and once a strong wind occurs i.e. $v = 10$–15 (m/s), a' and b' take the values of 30 (m) and 15 (m) respectively.

Once the scattering ellipse (circle) is specified, all cells locating inside or intersecting with the ellipse (circle) are the long-range neighbors of a fire cell.

4.4. Rules

Similar to the neighborhood setting, there are 2 rules for the 2 fire-spread patterns.

4.4.1. Short-Range Fire-Spread. The short-range fire-spread rule, i.e. whether or not cell j within the short-range neighborhood of fire cell i can be ignited by its radiation and convection, is performed using the ignition probability of cell j. The probability is given by the short-range ignition judgment index SF_{ij} defined by:

$$SF_{ij} = P(B_j) \cdot P(D_j) \cdot P(W) \cdot P(d_{ij}) \cdot P(S_i) \tag{5}$$

where

B_j is the structure parameter of cell j, and $P(B_j)$ is a ignited ability factor for different structures by radiation or convection. In relation to the 3 structure types mentioned in Section 4.2, the values of $P(B_j)$ are given as: (I) wooden = 1.0, (II) fire-prevention wooden = 0.8 and (III) fire-proof = 0.6.

D_j is the damage parameter of cell j by war or earthquake, and $P(D_j)$ is a influence factor of different damage types to fire-spread. In common, the damage to buildings under war or earthquake can be classified into 3 levels: (I) serious damage: the building cannot be repaired due to collapse or serious destructions; (II) moderate damage: the building can be repaired due to slight destructions; and (III) good condition: the building needs no repairs with no destructions. If a building suffers from moderate damage, such as a failed exterior wall, its contents would be exposed, and it is easier to be ignited. However, if a building is collapsed by shake, the debris would bury the contents and restrict the supply of air to fire, and fire-spread would slow down. Therefore, the values of $P(D_j)$ are given as: (I) serious damage = 0.6, (II) moderate damage = 1.0, (III) good condition = 0.9.

W is the weather condition parameter, and $P(W)$ is a influence factor of different weather conditions to fire-spread. In general, weather conditions can be classified into 3 types: (I) disadvantageous conditions: sunshine, torridity, dry and gales; (II) neutral conditions: sunshine, mild gale, and some humidity; (III) advantageous conditions: cloudy sky, rain, snow and high humidity. In corresponding to the 3 types of weather conditions, the values of $P(W)$ are given as: (I) disadvantageous = 1.0, (II) neutral = 0.8, (III) advantageous = 0.4.

d_{ij} is the shortest distance from fire cell i to cell j, and $P(d_{ij})$ is a distance factor affecting fire-spread, which decreases linearly with the ratio of d_{ij} to d_{jB}, the closest distance from cell j to the boundary of spread ellipse in the same direction of d_{ij} as shown in Figure 4.
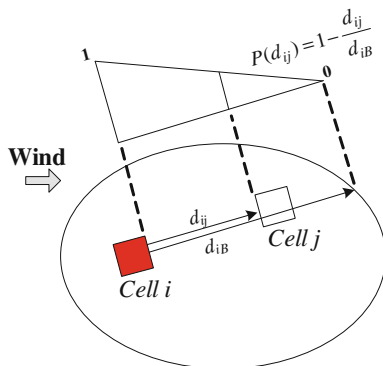
Figure 4. The value setting of $P(d_{ij})$.

$$P(d_{ij}) = 1 - \frac{d_{ij}}{d_{iB}} \tag{6}$$

S_i is the state parameter of cell i, and $P(S_i)$ is an ability factor of different states to spread fire to other cells. Since only state {3} and {4} have abilities to spread fire outside, the values of $P(S_i)$ are given as follows: state {3} = 0.4, and state {4} = 1.0. As for the other states, i.e. {0}, {1}, {2} and {5}, the values of $P(S_i)$ are all equal to 0.

4.4.2. Long-Range Fire-Spread. Similar to the short-range fire-spread, the long-range fire-spread rule is also performed using the ignition probability of cell j within the long-range neighborhood of fire cell i by its released firebrands. The probability can also be given by the long-range ignition judgment index LF_{ij} calculated for all long-range neighborhood cells of fire cell i. However, comparing with SF_{ij}, LF_{ij} is more difficult to calculate due to the complicated process of firebrand spotting.

As discussed in Section 4.3.2, the occurrence of ignition by a firebrand depends on several conditions, while reflecting all these conditions is virtually impossible. To simplicity, 3 key elements are taken into account in modeling LF_{ij}, i.e. (I) the number of firebrands released from a fire cell, (II) the location of a firebrand lofted to by fire plume, and (III) the ignition probability of a firebrand when landing on ground.

Using the 3 elements above, the ignition probability of the cell j caused by the k-th firebrand released by the fire cell i is formulated as:

$$P_k = P_{B,k} \cdot P_{G,k} \quad (k = 1 \sim n) \tag{7}$$

where n is the number of firebrands released by cell i with the escaped time t_r after fire fully developed; $P_{B,k}$ is the scattering probability of a firebrand from cell i to cell j; $P_{G,k}$ is the ignited probability of cell j by a landed firebrand.

Considering the ignition by a firebrand is independent from the others, the short-range ignition judgment index LF_{ij} of cell j by fire cell i can be predicted using the following equation.

$$LF_{ij} = 1 - \prod_{k=1}^{n} (1 - P_k) \tag{8}$$

4.4.2.1. The Released Number of Firebrands. Based on Yoshioka et al. [23], the brands are released only during the fully developed phase of buildings. Even till now, the exact calculation model for the released number of firebrands has not been figured out due to its complication. To simplicity, using Waterman data for the experiments with a 91 ft^2 roof section with a 45° roof pitch, 1 in. lumber sheathing, and 235 lb. asphalt shingles, and different applied wind pressures, the relationship between the number of firebrands released per m^2, N_A, and wind speed (m/s), v, was developed as follows [24]:

$$N_A = 306.77 e^{(0.1879 * v)} \tag{9}$$

Meanwhile, it is assumed that the number of brands released from a fire building with A m^2 floor area after fire full-development is drawn from a Poisson distribution as below:

$$\begin{cases} P\{N(t_r) = n\} = \dfrac{(N_t \cdot t_r)^n}{n!} \cdot e^{-N_t \cdot t_r} \\ N_t = \dfrac{N_A \cdot A}{t_3 + t_4} \end{cases} \tag{10}$$

where N_t is the time density of released firebrand number, t_3 is the time interval from state {3} to {4}, and t_4 is the time interval from state {4} to {5}.

Based on the Waterman [24] and other data, 3 brand sizes, i.e. fine, medium, and coarse, were defined, and corresponding distributions of brands among the 3 size categories were estimated (Table 5). Using this table, a firebrand released by a fire cell would randomly select a size category according to the percentage of the sizes. Then, the brand's area, thickness and density would also be chosen randomly in the ranges according to its size category.

Table 5
Brand Information by Size Category [24]

Size	Brand area (cm^2)	Brand thickness (cm) d_p	Brand density (kg/m^3) ρ_P	Percentage of brands (%)	Probability of ignition of wood
Fine	0.13–1.29	0.25–0.76	50–200	71	0
Medium	1.29–6.45	0.76–1.02	50–200	27	0.005
Coarse	6.45–58.06	1.02–1.78	50–200	2	0.020
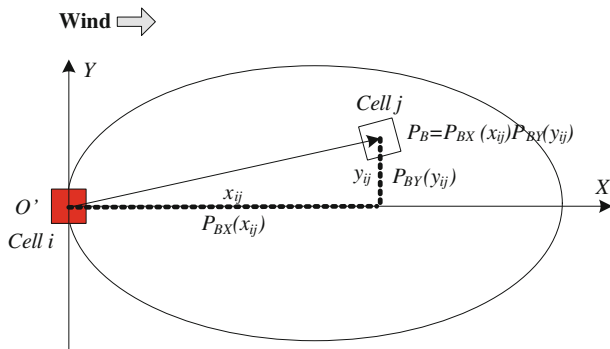
Figure 5. The value setting of $P_B(x_{ij}, y_{ij})$.

Since the release of firebrands only occurs during the full-developed phase, the firebrands are generated from fire cell i with the state {3} and {4}, and the number n of brands with the elapsed time t_r can be given through the stochastic calculation from Equation 10. Otherwise, if the cell i is in state {0}, {1}, {2} and {5}, no firebrands are released.

4.4.2.2. The Scattering Probability of a Firebrand. The scattering probability $P_{B,k}$ of the k-th firebrand is described incorporating the results of the numerical simulation on the transport behaviors of the disk-shaped firebrands. Specifying the concerns of fire-involved cell (i.e. fire cell i with state {3} and {4}) to be the coordinate of origin O', the scattering probability P_B of a firebrand from cell i to cell j can be divided into 2 parts: X-axis (i.e. leeward direction) scattering probability $P_{BX}(x_{ij})$ and Y-axis (i.e. lateral direction) scattering probability $P_{BY}(y_{ij})$ (Figure 5).

As discussed above, in the presence of wind, the X-axis scattering of firebrand satisfies as a log-normal distribution and the Y-axis scattering satisfies as a normal distribution. Thus, the overall scattering probability P_B can be given by a product of $P_{BX}(x_{ij})$ and $P_{BY}(y_{ij})$, which is [9]:

$$P_{B,k} = \left[P_{BX}(x_{ij}) \cdot P_{BY}(y_{ij}) \right]_k \tag{11}$$

and

$$\begin{cases} P_{BX}(x_{ij}) = \dfrac{1}{\sqrt{2\pi}\sigma_{L,X}x_{ij}} \exp\left\{ -\dfrac{(\ln x_{ij} - \mu_{L,X})^2}{2\sigma_{L,X}^2} \right\} \\[4mm] P_{BY}(y_{ij}) = \dfrac{1}{\sqrt{2\pi}\sigma_Y} \exp\left\{ -\dfrac{(y_{ij} - \mu_Y)^2}{2\sigma_Y^2} \right\} \end{cases} \tag{12}$$

where $\mu_{L,X}$ and $\sigma_{L,X}$ are the mean and standard deviation of the natural log of the transport distance in X-axis respectively. Whereas for Y-axis, the mean transport

distance is zero, and only the standard deviation σ_Y is considered. Their values are given as follows [9].

$$
\begin{cases}
\mu_{L,X} = \ln\left[\dfrac{d\left(0.47B'^{2/3}\right)}{\sqrt{1 + (0.88B'^{1/3}/0.47B'^{2/3})^2}}\right], & \sigma_{L,X} = \sqrt{\ln\left(1 + (0.88B'^{1/3}/0.47B'^{2/3})^2\right)} \\
\mu_Y = 0, \quad \sigma_Y = 0.92d \\
B' = \dfrac{v}{(gd)^{1/2}}\left(\dfrac{\rho_p d_p}{\rho_0 d}\right)^{-3/4}\left(\dfrac{\dot{Q}}{\rho_0 c_d T_a g^{1/2} d^{5/2}}\right)^{1/2}
\end{cases}
\tag{13}
$$

where d is the length scale of cell, which is calculated by the square root of cell's floor area; B' is a dimensionless parameter; v is the wind speed (m/s); $\dot{Q}$ is the fire's heat release rate (kW); c_d is the heat capacity of gas (kJ/kg K); g is the acceleration due to gravity (m/s^2); ρ_0 and T_a are density (kg/m^3) and temperature (K) of air. Based on the research of Bryant and Mulholland [25], $\dot{Q}$ is estimated to be $1500 \times$ (fire area) kW.

In the absence of wind or slight wind, i.e. $v = 0$–5 (m/s), the X-axis and Y-axis scatterings of firebrand all satisfy a same normal distribution as follows:

$$
\begin{cases}
P_{BX}(x_{ij}) = P_{BY}(y_{ij}) = \dfrac{1}{\sqrt{2\pi}\sigma}\exp\left\{-\dfrac{(z-\mu)^2}{2\sigma^2}\right\}, & (z = x_{ij} \text{ or } z = y_{ij}) \\
\mu = 0, \quad \sigma = 0.92d
\end{cases}
\tag{14}
$$

4.4.2.3. The Ignition Probability by a Landed Firebrand. The ignition probability of cell j by the k-th landed firebrand is mainly determined by 2 factors: the landed firebrand's size determining the ability of firebrand to ignite wooden materials, and the cell's structure parameter related with the ability of cell to be ignited by a firebrand. Therefore, the ignition probability of cell j by a landed firebrand can be defined as:

$$
P_{G,k} = P(s_k) \cdot P(B_j)
\tag{15}
$$

where $P(s_k)$ is the probability of the k-th landed firebrand with size s_k to ignite the wooden materials. For 3 sizes, i.e. fine, medium, and coarse sizes, the values of $P(s_k)$ have been given in Table 5. $P(B_j)$ is the probability of cell j with structure B_j to be ignited by a landed firebrand. To simplicity, 3 constants were employed to give the values of $P(B_j)$ for 3 structure types as: (I) wooden = 1.0, (II) fire-prevention wooden = 0.5, and (III) fire-proof = 0.

4.4.3. Comprehensive Effects. When mass fire occurs, the un-ignited cell would be under the interacting influence of multiple fire cells and the simultaneous effect of

2 fire spread patterns. Considering such comprehensive effects, the fire spreading judgment index F_j of cell j can be given as the Equation 16 as below:

$$F_j = 1 - \prod_{t=r}^{m} \left(1 - SF_{tj}\right) \cdot \prod_{k=l}^{n} \left(1 - LF_{kj}\right), \ (c_j \in \{SN(c_r), \ldots, SN(c_m)\},$$
$$c_j \in \{LN(c_l), \ldots, LN(c_n)\}), \tag{16}$$

where c represents a cell, $SN(c_t)$ is the short-range neighborhood of a fire cell c_t and $LN(c_k)$ is the long-range neighborhood of a fire cell c_k. $\in$ means 'within', i.e. the cell located within the short-range neighborhood or long-range neighborhood of a fire cell.

4.5. The Process of Fire Spread Simulation with CA Model

The flow of fire spread simulation with CA model is shown in Figure 6, and the detailed procedure can be executed as follows:

(1) Suppose a fire outbreak in a building, i.e. select a cell to be ignited by changing its state from {0} to {1} and setting its fire duration time t_c to 0.
(2) Start simulation with the initial simulation time $t = 0$.
(3) Increase the simulation time by a time interval (i.e. $t = t + dt$) and judge whether the current time t is up to the end time t_e. If $t > t_e$, the simulation is terminated.
(4) Otherwise, the wind conditions (speed and direction) are reset for the current time t. Then, 2 steps are performed in sequence.
(5) The first step is to transit the state of cells. In detail, pick out the cells with state {1}, {2}, {3} and {4}, and reset fire duration time for each selected cell as $t_c = t_c + dt$. If t_c of cell with state {1} exceeds the flashover time t_f, the cell's state will change from {1} to {2}; if t_c of cell with state {2} exceeds the full-development time t_d, the cell's state will change from {2} to {3}; if t_c of cell with state {3} exceeds the structure fire time t_s, the cell's state will change from {3} to {4}; if t_c of cell with state {4} exceeds the collapse time t_p, the cell's state will change from {4} to {5}.
(6) The second step is to apply 2 neighborhoods and rules in cells. Firstly, pick out the cells with state {3} and {4}, and select their short-range and long-range neighborhood cells with state {0}. Then, both SF and LF are calculated for each selected cell under the effect of multiple fire cells. After that, the comprehensive fire spread judgment index F is calculated based on SF and LF for each selected cell. A random number R are generated in [0, 1] for each cell and compared with F. If $F > R$, the cell is thought to be ignited, and its state changes from {0} to {1} and its fire duration time t_c is set to 0.
(7) Increase time interval again and perform the steps from (4) to (6) repeatedly until the simulation time is up.
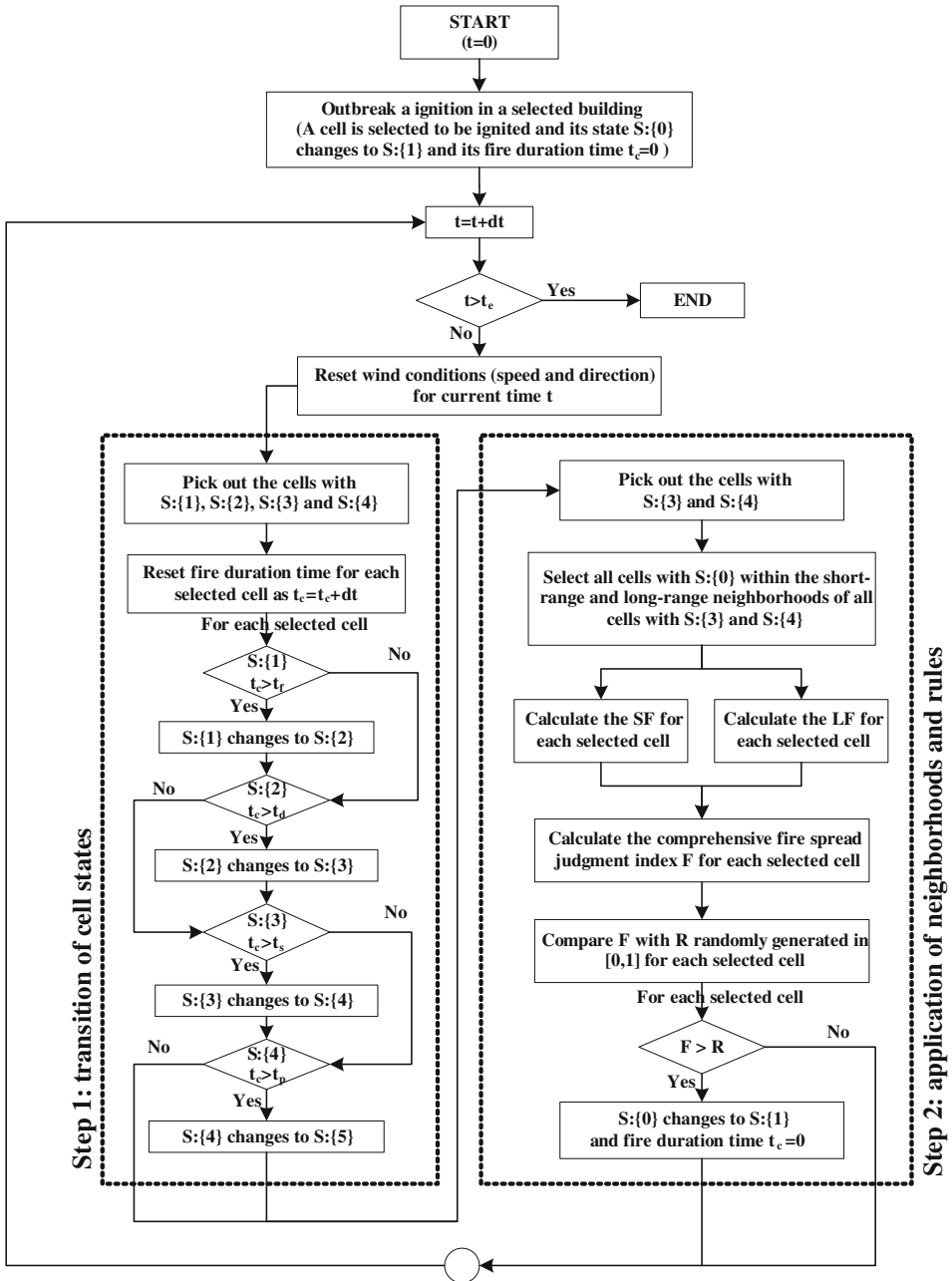
Figure 6.   The flow of urban fire spread simulation with CA model.

5. Development of the Integrated GIS-CA-Fire Tool

5.1. *The Integration of GIS and CA*

A Geographic Information System (GIS) is a system for capturing, storing, analyzing and managing spatial referenced data. With its powerful geographical analysis and visualization capacities, GIS is currently widespread in natural resources management, environmental impact assessment, cartography, criminology, urban planning etc. In the recent years, GIS has been widely applied in the field of urban hazard analysis, such as hazard assessment, simulation, prediction, emergency response and etc. As one of urban hazards, fire-spread process in urban densely built areas can also be simulated on the GIS platform. For this purpose, the integrated tool of GIS and CA for urban fire-spread simulation, named GIS-CA-fire tool is developed. To be specific, the integrated GIS-CA-fire tool was developed using ArcEngine and C# programming language.

Figure 7 shows the detailed seamless integration process of GIS and CA. Firstly, a vector building layer (shapefile format), where each feature represents a building with its geographic location, geometry and attributes, is loaded and displayed. Considering that a building is a cell, the features are extracted from the layer using ArcEngine's API and converted to the cells of CA with their attributes. Then, the CA fire spread simulation program is executed. After each increasing time interval, the state of cells may change to represent fire-spread under the application of neighborhoods and rules. To display such a dynamic fire spread process in a GIS map, different color symbols for different states of cell are
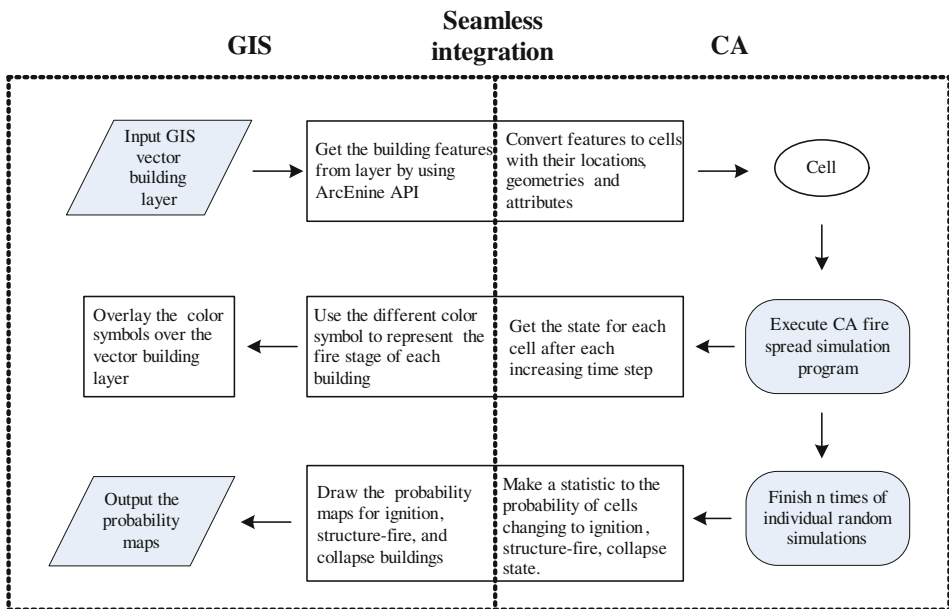

Figure 7. The seamless integration of GIS and CA.

overlaid on the building layer. Due to the stochastic character of CA, individual random simulation needs to be performed for several times to obtain a steady simulated result. After n times of individual simulations, the probabilities (or frequencies) of each cell changing to ignition, structure-fire and collapse states would be calculated. To display such 3 probabilities of buildings after fire-spread simulations, 3 classified-rendered probability maps are drawn. Such maps will play an important role in the loss assessment by fire-spread.

5.2. Development of the User Interfaces

The intuitive, flexible, and user-friendly interfaces are developed to make the model easy to a wider audience who might not have GIS expertise (e.g. fire managers, city planners, or researchers). This allows the end-user to take advantage of the essentials of GIS and modeling functionalities without interacting with the GIS tools. Figure 8 shows the main UI of GIS-CA-fire tool, which is simple and easy enough to operate.

In the main UI, there is an important component, named simulation control panel, which gathers all the operations of simulation. It consists of four tabs: (a) setting tab, (b) option tab, (c) simulation center tab, and (d) dynamic simulation tab (Figure 9). In the setting tab, 3 settings are to be performed, i.e. (1) selecting a building layer and choosing its attribute fields, (2) selecting a weather condition for simulation, and (3) setting the wind conditions (wind speed and direction) per simulation hour. Option tab is to finish (1) initial ignitions' selection, (2) fire-spread patterns' selection, and (3) loss parameters' setting. Simulation center tab is
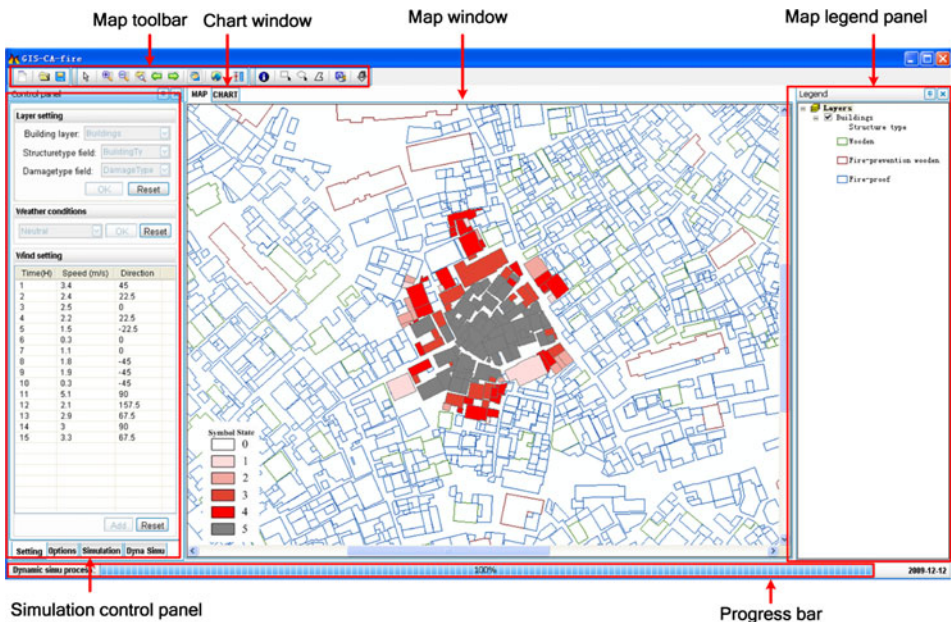
Figure 8.   The main UI of GIS-CA-fire tool.
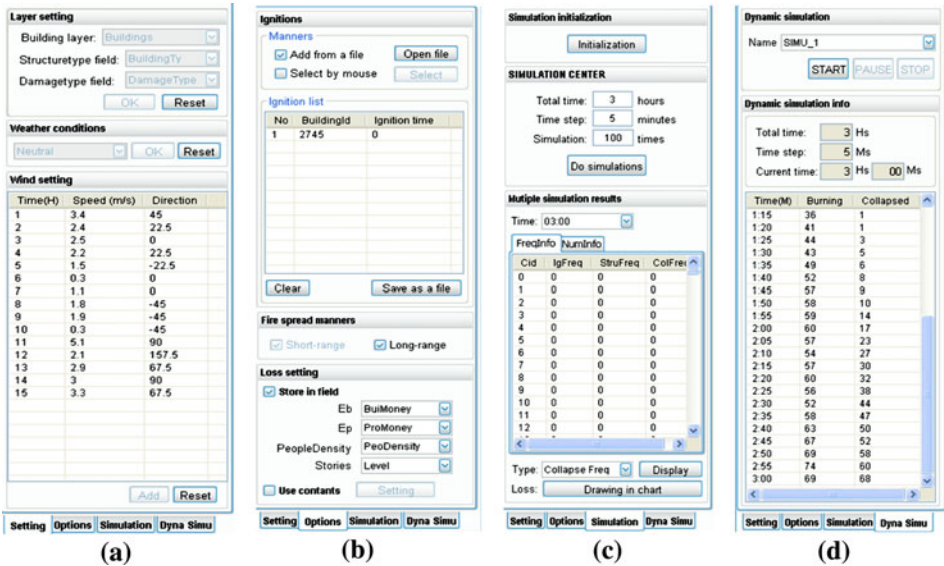
Figure 9. Four tabs of simulation control panel. (a) Setting tab, (b) options tab, (c) simulation tab, and (d) dynamic simulation tab.

the most key one that can perform fire-spread simulations after the settings of time interval, total simulation time and the times of individual simulation, and then produce the probability maps and fire-prone losses charts. In the final tab, i.e. dynamic simulation tab, an animation of dynamic fire-spread process is shown and its corresponding information is presented in a list.

6. Validation

In order to verify the newly developed CA fire-spread model, a simulation of fire-spread at a real site was performed with the GIS-CA-fire tool. The site was located nearly to a hospital in Kobe city after Hanshin Earthquake (1995, Japan). The ignition broke out at 5:47 a.m. after shake and the fire-spread lasted for 15 h [14]. According to the local meteorological records, the wind directions and speeds during 15 h are listed as Table 6 [14].

Notably, because the inherent stochastic process was built into the CA model, even if simulation is executed as little as 2 times, one result would differ from the other. Therefore, if we attempt to obtain a steady simulation result, individual simulation needs to be carried out for many times. One simulation can just output one sample. Although it is not easy to obtain an optimal sample number mathematically, in consideration of the practical utility of a quick response time in simulation calculation for disaster mitigation, 100 samples are often enough for the stable statistical results.

Table 6
Wind Direction and Speed from 5 O'clock to 20 O'clock (for 15 h) [14]

Time	Wind direction	Wind speed (m/s)
5:00	ENE	1.6
6:00	NE	3.4
7:00	ENE	2.4
8:00	E	2.5
9:00	ENE	2.2
10:00	ESE	1.5
11:00	E	1.3
12:00	E	0.1
13:00	SE	1.8
14:00	SE	1.9
15:00	SE	0.3
16:00	N	5.1
17:00	WNW	2.1
18:00	NNE	2.9
19:00	N	3.0
20:00	NNE	3.3

*Note*: 'N' is North, 'S' is South, 'E' is East, and 'W' is West.

After 100 times of individual simulations, 2 kinds of probability maps were generated to respectively display the probabilities (or frequencies) of cell changing to state {1} and state {5}, i.e. ignition and collapse. Figure 10 shows 4 pairs of comparisons, one is the fire-spread map from local observations [14] and the other is the ignition and collapse probability maps from simulations, at 4 local observed times: 7:00, 10:00, 13:00 and 20:50. Table 7 presents the quantity comparison of ignited and collapsed buildings between observations [14] and simulations.

From the figure, it is obvious that the shape of fire-spread from simulations well matches the real shape from observations. Moreover, from the table, it is clear to see that the quantities (mean quantities and their confident intervals) of ignited and collapsed buildings from 100 times of simulations also match the real numbers from observations perfectly. Therefore, it is convincing that the newly developed CA fire-spread model is reliable to be used in simulating fire-spread in urban areas.

Moreover, it took only about 45 min to finish the 100 times of simulations and gave all the statistical results. It is faster than the fire-spread simulation (more than 3 h) to the same site by using the pure physically based models.

7. Loss Assessment Model

The losses, including *economic losses* and *life losses*, by fire-spread are all considered in the GIS-CA-fire tool. Economic losses usually consist of direct and indirect economic losses, but in this paper only direct economic losses are taken into account.

7:00 (fire spreading for 1 hour and 10 minutes)

10:00 (fire spreading for 4 hours and 10 minutes)
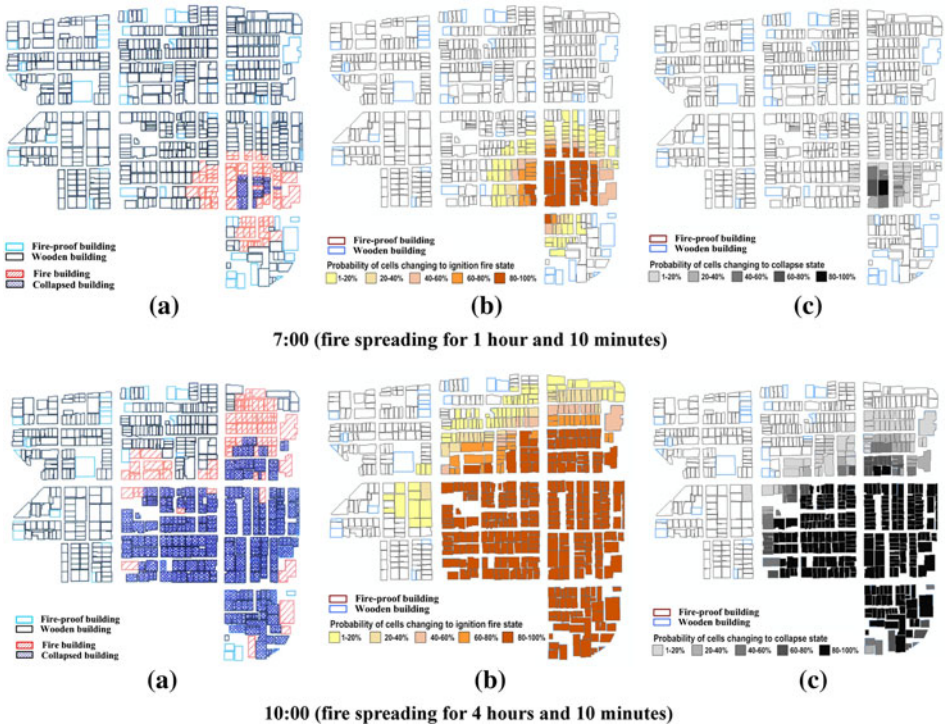
Figure 10. Comparison between the observed maps [14] and simulated probability maps. (a) Observed map, (b) ignition probability map, and (c) collapse probability map.

7.1. *Direct Economic Losses Assessment*

The direct economic losses include: (I) the cost to rebuild burnt cells (buildings) and (II) the cost of the indoor properties within burnt cells (buildings). The detailed calculation to direct economic losses is given as below.

$$L_E = \sum_{i=1}^{N} \left[(0.2P_{ig} + 0.6P_{stru} + 0.2P_{col})_i \cdot (E_b + E_p)_i \cdot A_i \right] \qquad (17)$$

where L_E denotes the total economic losses for a fire burnt area; N is the total number of all burnt cells (buildings) in the area; E_b is the cost per m^2 to rebuild the i-th burnt cell (building); E_p is the cost per m^2 of the properties inside the i-th burnt cell (building). The values of E_b and E_p are not fixed, and they will vary with the economic conditions of studied city. Therefore, before losses assessment, the economic level of studied city need to be investigated and the averaged values of E_b and E_p need to be figured out. A_i is the total constructed area (m^2) of the i-th burnt cell (building), and it is nearly equal to the product of its floor area and

13:00 (fire spreading for 7 hours and 10 minutes)

20:50 (fire spreading for 15 hours)
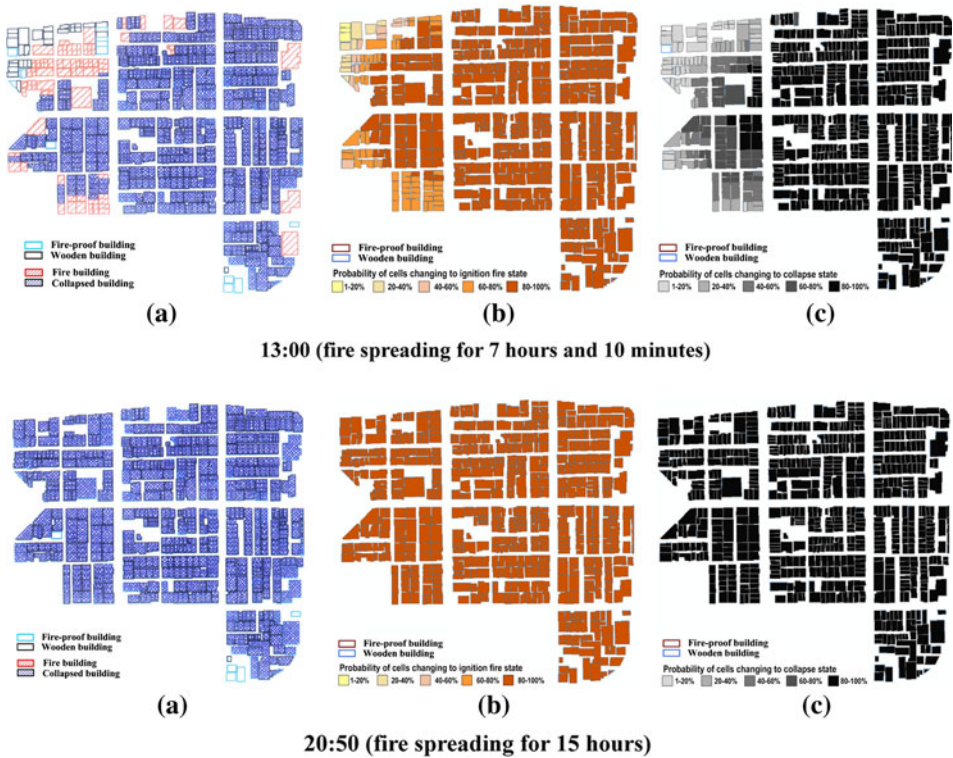
Figure 10. continued.

stories; P_{ig}, P_{stru} and P_{col} are the ignition, structure-fire and collapse probabilities of the *i*-th burnt cell (building) after 100 times of individual simulations.

7.2. Life Losses Assessment

Usually, it takes some time for fire to spread from initial ignited building to other buildings. Except the initial ignited building, people have enough time to escape from the building before the reach of fire. Therefore, the life losses would be small and just confined in the initial ignited building. But under the background of war or earthquake, the situations would be different. Especially, earthquake would suddenly shake down the buildings to bury people in the debris. Once fire breaks out, all buried people, whether they are dead or injured, cannot be rescued out timely before the reach of fire. Therefore, in case of fire following earthquake, all dead and injured people by shake become the fatalities by fire, which can be calculated as follows [26].

$$N_P = (A_1 R_1 + A_2 R_2 + A_3 R_3)\rho \tag{18}$$

where N_P is the total number of the fatalities in a fire burnt area; A_1, A_2 and A_3 are the floor areas (m^2) of collapsed, seriously damaged and moderately damaged

Table 7
Quantity Comparison of Ignited and Collapsed Buildings Between Observations [14] and Simulations

	Observations		Simulations															
			Quantity of ignited buildings							Quantity of collapse buildings								
	Quantity of ignited	Quantity of collapse	Quantity of buildings for different ignition probability intervals					Mean	95% confident	Quantity of buildings for different collapse probability intervals					Mean	95% confident
Time	buildings	buildings	0% to 20%	20% to 40%	40% to 60%	60% to 80%	80% to 100%	quantity	interval	0% to 20%	20% to 40%	40% to 60%	60% to 80%	80% to 100%	quantity	interval
7:00	70	9	61	19	12	10	47	67	[64, 70]	26	5	7	1	1	8	[7, 9]
10:00	374	298	66	34	20	27	347	379	[372, 387]	55	22	23	29	256	290	[285, 295]
13:00	647	575	3	7	16	55	608	643	[634, 652]	46	24	40	49	528	584	[574, 593]
20:50	683	683	0	0	0	0	689	689	[689, 689]	0	0	0	0	689	689	[689, 689]

Table 8
Rate of Death and Injury Under the Earthquake [26]

Damage level	Intact	Slight	Moderate (R_1)	Serious (R_2)	Collapse (R_3)
Death rate	0.0	0.0	0.00001	0.001	0.017[a]
Injury rate	0.0	0.0003	0.0034	0.034	0.89

[a] This value is for the daytime and 0.034 for the nighttime.

buildings in the burnt area, respectively; R_1, R_2 and R_3 are the sum of death and injury rate for the buildings encountering the collapse, serious damage and moderate damage (Table 8); ρ is the average density of population (per m^2 building floor area) in the burnt area.

7.3. *Case Study on Loss Assessment Using GIS-CA-Fire Tool*

In this study case, the GIS-CA-fire tool was applied in a small district in Xiamen City, China. This district has several characters that will easily break out mass fire-spread as it includes a great proportion of wooden and wooden-frame buildings, small gap among buildings and lacks of fire-breaks to stop fire-spread.

After 100 times of individual simulations of 3-h fire-spread in this district, the ignition, structure-fire and collapse probability maps were produced respectively by the GIS-CA-fire tool as shown in Figure 11. Meanwhile, on basis of the probability maps above, the charts of direct economic losses, life losses and quantity of ignited and collapsed buildings were produced as shown in Figure 12.

8. Summary

Mass fire-spread in urban densely built areas is dangerous urban disaster, which would bring great losses to humans due to its large fire burnt area. The aim of this paper is to develop a fire-spread model based on irregular coarse CA to simulate the process of mass fire-spread and assess its losses. The main progresses of this paper are summarized as below.

(1) Analyzed the process of urban fire-spread and pointed out 2 sub-processes: (I) fire-development in a single building and (II) fire spread among buildings. During the sub-process (I), fire building experiences 5 key stages: ignition, flashover, full-development, structure-fire and collapse. During the sub-process (II), 2 spread patterns are involved in fire-spread among buildings, i.e. (I) short-range direct flame contact, radiative and convective spread and (II) long-range firebrand spotting.

(2) Proposed a CA model to simulate mass fire-spread process in urban densely built areas. In order to avoid the shortcomings of regular grid as cell, irregular coarse cell, i.e. a building as a cell directly, is employed in CA model. 6 states of cell are proposed in corresponding to 5 fire stages in a single building. Meanwhile, the time intervals for each state are given from the experts'

Figure 11. Three types of probability maps after 3-h fire-spread simulation. (a) Ignition probability map, (b) structure-fire probability map, and (c) collapse probability map.
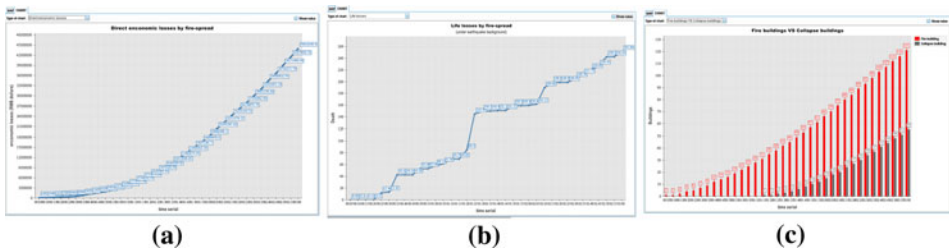
Figure 12. Three types of charts after 3-h fire-spread simulation. (a) Chart of direct economic losses, (b) chart of life losses, and (c) chart of ignited and collapsed buildings.

suggestions. Moreover, 2 types of neighborhood and rule settings for 2 fire-spread patterns are developed respectively. Finally, a detailed executing flow to apply new CA model for simulating urban fire spread is presented.

(3) Developed a seamlessly integrated GIS-CA-fire tool for simulating urban mass fire-spread with friendly user interfaces, advanced spatial analysis functionalities and institutive graphic display.

(4) To validate the newly developed fire-spread model, the GIS-CA-fire tool was used to perform 100 times of random individual simulations of fire-spread at a real site in Kobe City, Japan. Through the comparison with local observations, it is proved that the new model is reliable to simulate fire-spread in urban areas.

(5) Formulated both economic and life loss assessment models caused by fire-spread.

On the other hand, there is also one issue left for future studies. In this paper, it is assumed that urban mass fire would spread freely without suppression. But as we all know, the local fire-fighting activities would play an important role in stopping fire-spread. Therefore, the influence of urban fire-fighting activities to fire-spread needs to be modeled in the future work.

Acknowledgments

References

1. Pittts WM (1991) Wind effects on fires (review). Prog Energy Combust Sci 17:83–134
2. Scawthorn C, Eidinger JM, Schiff AJ (2005) Fire following earthquake. ASCE Press, Reston
3. Chen W, Scawthorn C (2003) Earthquake engineering handbook. CRC Press, Boca Raton
4. Rothermel RC (1983) How to predict the spread and intensity of forest and range fires. General Technical Report INT-143
5. Japan Association for Fire Science and Engineering (1997) Handbook of fire. Kyoristu Publishing, Tokyo (In Japanese)
6. Namba J, Yasuno K (1986) A study on the fire spread model of wooden buildings in Japan. In: First safety science—proceedings of the first international symposium, pp 881–890
7. Himoto K, Tanaka T (2000) A preliminary model for urban fire spread-building fire behavior under the influence of external heat and wind. In: Thirteenth meeting of the UJNR panel on fire research and safety, vol 2, pp 309–319
8. Himoto K, Tanaka T (2002) A physically-based model for urban fire spread. In: First safety science—proceedings of the seven international symposium, pp 129–140
9. Himoto K, Tanaka T (2008) Development and validation of a physics-based urban fire spread model. Fire Saf J 47:477–494
10. Lee S, Davidson R (2008) Modeling different modes of post-earthquake fire spread. In: Proceedings of the 14th world conference on earthquake engineering
11. Cousins W, Heron D, Mazzoni S (2002) Estimating risks from fire following earthquake, Client Report 60. Institute of Geological and Nuclear Sciences, New Zealand
12. Ohgai A, Gohnai Y, Watanabe K (2007) Cellular automata modeling of fire spread in built-up areas—a tool to aid community-based planning for disaster mitigation. Comput Environ Urban Syst 31:441–460
13. Fan W et al (1995) Concise study course of fire. University of Science and Technology of China Press, Hefei, China (In Chinese)
14. Fire Department of Kobe City (1996) Fire Situation following Hyogo-ken Nambu in Kobe City. Tokyo Press, Kobe (In Japanese)
15. Proterie B, Zekri N et al (2007) Modeling forest fire spread and spotting process with small world networks. Combust Flame 149:63–78
16. El-Yacoubi S, El-Jai A (2002) Cellular automata modelling and spread ability. Math Comput Model 36:1059–1074
17. El-Yacoubi S, El-Jai A (2003) Notes on control and observation in cellular automata models. WSEAS Trans Comput 2:1086–1109
18. Toffoli T (1984) Cellular automata as an alternative to differential equation in modeling physics. Physica D 10:117–127

19. Chopard B, Droz M (1998) Cellular automata modeling of physical systems. Cambridge University Press, Cambridge
20. Gaylord RJ, Nishidate K (1996) Modeling nature. Cellular automata simulations with mathematica. Springer-Verlag, New York
21. Wolfram S (1994) Cellular automata and complexity: collected paper. Addison-Wesley Publishing Company, Reading
22. Garzon M (1995) Models of massive parallelism. Analysis of cellular automata and neural networks. Springer-Verlag, Berlin
23. Yoshioka H, Hayashi Y, Masuda H, Noguchi T (2004) Real-scale fire wind tunnel experiment on generation of firebrands from a house on fire. Fire Sci Technol 23(2): 142–150
24. Waterman T (1969) Experimental study of firebrand generation, Project J6130. IIT Research Institute, Chicago, IL
25. Bryant R, Mulholland G (2008) A guide to charactering heat release rate measurement uncertainty for full-scale fire tests. Fire Mater 32:121–139
26. Tang A, Wen A (2009) An intelligent simulation system for earthquake disaster assessment. Comput Geosci 35(5):871–879